Final-state effects in photoemission experiments from graphene on Ni(111)

Haarlammert, Thorben; Bignardi, Luca; Fecher, Gerhard; Rudolf, Petra; Zacharias, Helmut; Winter, C

Published in:
European Physical Journal B

DOI:
10.1140/epjb/e2013-40044-1

Publication date:
2013

Eur. Phys. J. B (2013) 86: 225
DOI: 10.1140/epjb/e2013-40044-1

THE EUROPEAN PHYSICAL JOURNAL B

Regular Article

Final-state effects in photoemission experiments from graphene on Ni(111)

Thorben Haarlammert[1], Luca Bignardi[2], Carsten Winter[1], Gerhard Fecher[3], Petra Rudolf[2,a], and Helmut Zacharias[1,b]

[1] Physikalisches Institut, Westfälische Wilhelms-Universität Münster, Wilhelm-Klemm-Strasse 10, 48149 Münster, Germany
[2] Zernike Institute for Advanced Materials, University of Groningen, Nijenborgh 4, 9747AG Groningen, The Netherlands
[3] Institut of Inorganic and Analytical Chemistry, Johannes Gutenberg University Mainz, Duesbergweg 10-14, 55128 Mainz, Germany

Received 21 January 2013 / Received in final form 18 March 2013
Published online 20 May 2013 –

Abstract. Photon-energy dependent photoemission experiments using high harmonic radiation as a tunable photon source on epitaxially grown graphene on a Ni(111) substrate are presented. A resonance in the photoemission cross section for the σ and π states of graphene was observed and compared to a simple model for the determination of photoemission cross sections of free standing graphene, pointing out the role of the interaction of graphene with the nickel substrate.

1 Introduction

Graphene has attracted considerable scientific interest and attention in the last years. Its peculiar 2D crystalline lattice is responsible for several surprising electronic and structural properties that have been widely investigated [1–3]. The relevant electrical and optical properties are caused by the π band dispersion around the K point of the Brillouin zone, which is linear when the graphene is not interacting with a substrate [4]. However, the technological future exploitation of graphene requires a detailed knowledge of the graphene-metal interfaces, whose electronic properties can significantly differ from those of free-standing graphene, as a consequence of the interaction with the metal [5,6].

Ultraviolet photoelectron spectroscopy (UPS) is a tool widely used for the investigation of the electronic structure of this material [7] and its interaction with the underlying substrate. In this work we apply high harmonic generation of ultrashort laser pulses as a tunable and polarized tabletop photon source in the extreme ultraviolet (EUV) spectral region. The tunability of this photon source enables the measurement of relative photoemission (PE) cross sections of various occupied electronic states, employing photons with an energy between of $h\nu = 23.6$ eV and 53.6 eV. The PE spectra of the valence band of graphene grown on a Ni(111) substrate by chemical vapour deposition (CVD) have been collected and a distinct profile for the PE cross section was observed for the σ and the π bands of graphene. These experimental results were compared to tight-binding calculations of the band structure.

[a] e-mail: p.rudolf@rug.nl
[b] e-mail: hzach@uni-muenster.de

2 Experimental

Frequency conversion by high harmonics generation (HHG) of femtosecond visible laser pulses affords a tabletop source of stepwise tunable extreme ultraviolet (EUV) radiation. In noble gases like argon odd harmonic orders of the fundamental photon energy are generated, providing EUV pulses with femtosecond duration [8]. Laser intensities on the order of 10^{13}–10^{14} W/cm^2 are required to generate high harmonics in noble gases. In the setup employed for this experiment, a Ti:Sapphire laser system is used to generate ultrashort laser pulses with a pulse energy of about 1 mJ, a pulse duration of 30 fs [9] at 6 kHz repetition rate. These ultrashort pulses are focused onto an Ar gas target similar to the set-up of Spielmann et al. [10] for nonlinear frequency conversion. In the present experiments argon was employed as nonlinear medium, since it is the most efficient target for EUV photon energies between $h\nu = 20$ eV and 55 eV [11]. By rotating the direction of the linear polarization of the fundamental, the polarization of the harmonics is changed accordingly. A thin Al foil (100 nm thick) was used to block the fundamental light and additionally to stop the residual gas flow from entering the experimental chamber. The foil is nearly transparent for photon energies between $h\nu = 20$ and 70 eV and it can therefore be used to separate the generated EUV radiation from the fundamental beam. The odd harmonic orders of the fundamental photon energy are generated simultaneously. Therefore, a toroidal grating was used to select a specific harmonic order and thus to change the energy of the photons employed for the photoemission experiment.

The PE spectra were acquired in an ultrahigh vacuum (UHV) chamber with a base pressure of 2×10^{-10} mbar.

The Ni(111) single crystal surface was prepared by several cycles of argon ion sputtering ($E_{ions} = 1$ keV) and subsequent annealing at high temperature (1080 K). The graphene layer was grown in-situ, following the chemical vapour deposition (CVD) procedure described in the literature [12], employing ethylene gas (purity 99.95%, Messer Gas) at 885 K. Due to the almost perfect matching of the Ni(111) and graphene surface lattice parameters, a $p(1 \times 1)$ pattern was observed with a low energy electron diffraction (LEED), suggesting that all graphene domains were oriented in the same fashion. Furthermore, this excludes the presence of nickel carbide crystalline domains, which might affect the growth of graphene on Ni depending on the temperature at which the hydrocarbons exposure takes place [13]. In fact, nickel carbide is characterized by a crystalline structure with a square symmetry, hence the corresponding diffraction pattern can easily be distinguished from the graphene one. LEED data collected at different positions of the sample revealed only patterns that could be attributed to the graphene layer, while no carbide domains were detected (not shown). This agrees with literature data [14] which demonstrate that the formation of nickel carbide is unfavorable at the temperature chosen for the growth.

Ultraviolet photoelectron spectroscopy (UPS) measurements using a commercial He-II discharge lamp and electron analyzer (Focus CSA 300) show at normal emission in an angle-integrated UPS spectrum, the π and σ bands of graphene, and thereby confirm the presence of graphene on the surface.

Photoemission spectra using the HHG source were acquired by means of a time-of-flight (TOF) detector. The electron flight time was measured in a field-free drift tube and the electrons were detected using a micro channel plate (MCP) detector. A total energy resolution of about 0.5 eV was achieved, limited by the finite energy bandwidth of the generated harmonics and by the time resolution of the TOF spectrometer. The EUV photon beam arrived on the sample with an incidence angle of ca. $\vartheta = 55°$ with respect to the surface normal. All spectra shown here were taken at normal emission, that is at the Γ point of the Brillouin zone of the graphene. The angular acceptance of the spectrometer is $\pm 2.5°$, which corresponds to an integration over $\Delta k_{\parallel} = 0.37\,\text{Å}^{-1}$ at $E_{kin} = 39.2\,\text{eV}$.

3 Results

Figure 1 presents photoemission spectra from graphene on Ni(111) taken with photon energies between $h\nu = 23.4$ eV (15th harmonic order) and 54.6 eV (35th harmonic order). The spectra were normalized to the secondary photoelectron background because of the unequal conversion efficiencies for different harmonic orders. In Figure 1a spectra taken with $\hat{p}$-polarized EUV radiation are reported. The zero binding energy (E_B) has been set to the Fermi level E_F. The most prominent structure derived from the $3d$ band of Ni can be recognized at about 1 eV below the

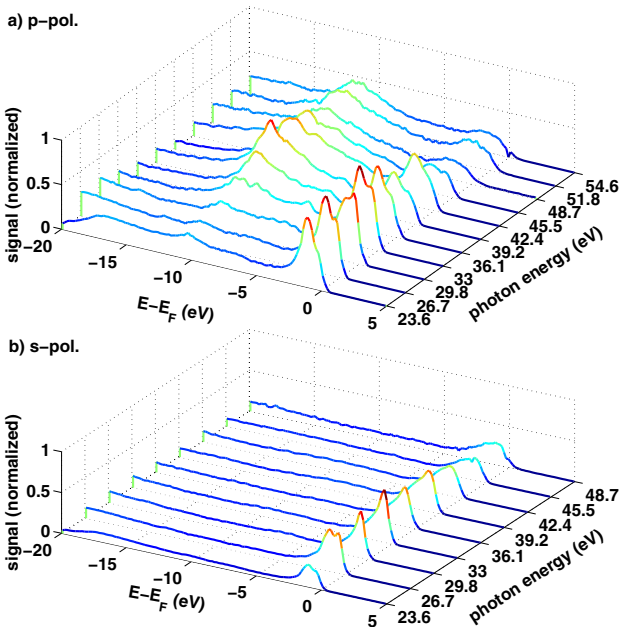

Fig. 1. Photoemission spectra of on graphene on Ni(111) with (a) $\hat{p}$- and (b) $\hat{s}$-polarized light, collected at normal emission, with various photon energies, as indicated.

Fermi level [15]. Additional structures are evident at binding energies of $E_B = -5.5$ eV and $E_B = -11$ eV and can be assigned to emission from the graphene σ and π bands, respectively. The position of the π states in the photoemission spectra at normal emission is shifted by about 3 eV towards higher E_B with respect to the graphene not interacting with any substrate [4]. The Ni substrate induced a shift in agreement with what was observed in earlier experiments [16,17]. Figure 1b shows analogous photoemission spectra taken with $\hat{s}$-polarized light, where one clearly distinguishes emission from Ni $3d$ bands. On the contrary, it is not possible to observe the structures belonging to π and σ bands of graphene, which are visible in photoemission with $\hat{p}$-polarized light only. This is due to the geometry of graphene bands and their selection rules for the photoionization [18,19].

The photoemission spectra taken with both $\hat{s}$- and $\hat{p}$-polarized light show important changes in intensity, related to the PE cross sections. In our experimental setup the photon flux cannot be recorded while collecting the photoemission spectra. Since the conversion efficiency strongly depends on the harmonic order selected for photoemission measurements, the spectra have to be normalized to the secondary photoelectron background to compare spectra taken at different photon energies. Therefore only the relative photoemission cross section can be measured with the method we employed [20]. Figure 2 shows the relative photoemission cross section of the graphene σ and π bands measured with various photon energies, as derived from the spectral intensities of Figure 1a. The profile of the photoemission cross section dependence on the photon energy of both bands shows a broad resonance. For the π state the maximum PE cross section in the experimentally accessible energy region is reached at a photon

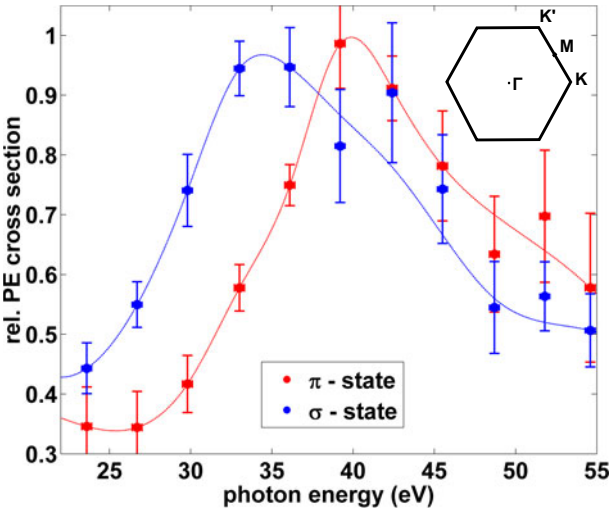

Fig. 2. Experimentally determined relative photoemission cross sections for the graphene σ and π bands, measured with various photon energies. The lines are guides for the eye.

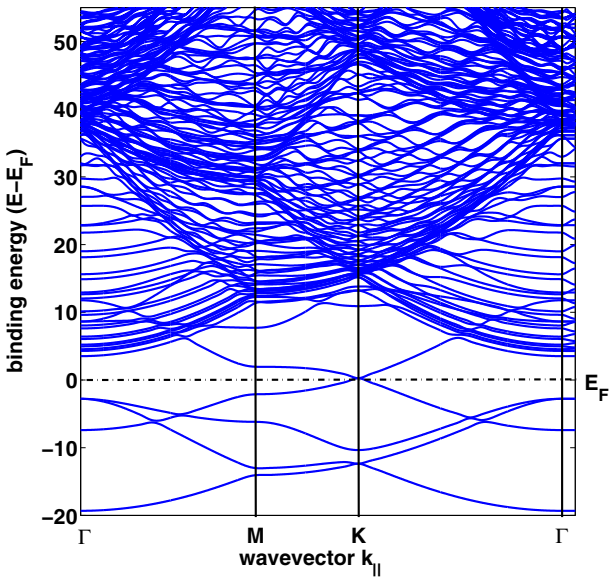

Fig. 3. Tight-binding simulation of the electronic band structure of free standing graphene.

energy of $h\nu = 39.2\,\text{eV}$, while that of the σ state occurs approximately at $h\nu = 34.0\,\text{eV}$. The two resonances are therefore spaced about 5 eV apart on the photon energy scale; this difference agrees very well with the difference in binding energy between π and σ states. Therefore we suggest that the maximum in the photoemission cross section for both bands is due to an increased density of final states.

4 Discussion

To understand the presence of such cross section maxima, the band structure for occupied and unoccupied states of a free-standing graphene was calculated with a tight-binding approach using standard methods. This includes atomic potentials with full crystal symmetry, Slater exchange and gradient corrections of the electron density. The results of this calculation are shown in Figure 3. The σ and π bands are found, at the Γ point of the Brillouin zone, at binding energies of $E - E_F = -4.8$ eV and $E - E_F = -7.4\,\text{eV}$, respectively. The Dirac point is observed at the K point of the Brillouin zone and the Fermi level is exactly crossing the vertex of the Dirac cone. The numerical results of the occupied band structure are in good agreement with literature data [4,21,22]. The distinctive feature of our calculation is that the energetically high unoccupied electronic states that have been taken into account because transitions from the π and σ bands were excited by high photon energies in the experiment. The unoccupied band structure has been calculated up to 55 eV above the Fermi level. A free electron-like dispersion is observed for most of the unoccupied electronic states. Unfortunately it is not possible to calculate the PE cross section directly from tight-binding simulations. Also the density of states cannot easily be extracted exactly from such calculations because the finite lifetime and, accordingly, the energy bandwidth of the electronic states can not be derived from the numerical data.

To obtain further information from the calculated band structure in Figure 3, we take a closer look at the number of unoccupied electronic states in the $\Gamma \rightarrow L$ direction of the Brillouin zone, i.e. the states involved in direct transitions from the Γ point to unoccupied energy states. This direction is orientated perpendicular to the sample surface and therefore responsible for the PE in the normal direction. In Figure 4 the number of unoccupied electronic states for each 0.5 eV energy interval above the Fermi level is plotted as grey colored bars. The total number is normalized to the maximum value, at an energy of $E - E_F = 38.5\,\text{eV}$. A relatively low number of electronic states per energy interval is observed for energies below $E - E_F = 35\,\text{eV}$. Increasing the energy, a sharp rise in the number of states is observed, reaching a maximum at $E - E_F = 38.5$ eV above the Fermi level, followed again by a fast decrease. This maximum indicates a high number of electronic states in a relatively narrow energy region. The energy bandwidth of the unoccupied electronic states of graphene was assumed to increase linearly with the energy of the state, ranging from 300 meV for states close to the Fermi level up to 2 eV for states at the highest energy considered. Of course this is a very rough assumption because the electronic lifetime in each state will depend on the specific electron energy and momentum. The resulting approximated density of states is plotted as a blue line in Figure 4. As expected from the number of electronic states mentioned before, the density of states shows a broad maximum at about 38.5 eV above the Fermi level.

Assuming that each PE cross section is proportional to the density of accessible unoccupied electronic states, the relative cross sections can be calculated. When comparing to the measured resonance, one has to bear in mind that the latter is broadened by the energy bandwidth of

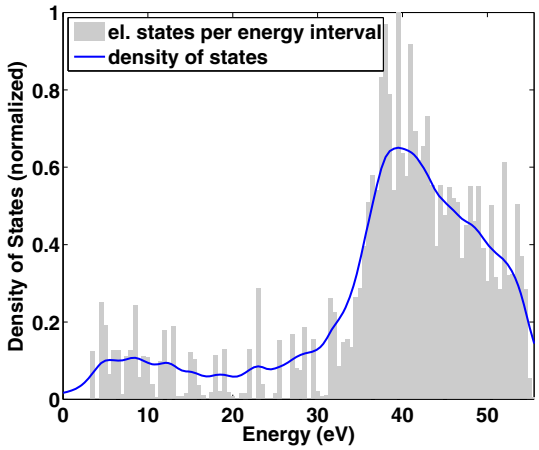

Fig. 4. Number of unoccupied electronic states in 0.5 eV energy intervals (grey). The calculated density of states assuming a 2 eV energy bandwidth for all states observed is plotted in blue. The zero of the bottom scale represents the position of the Fermi level.

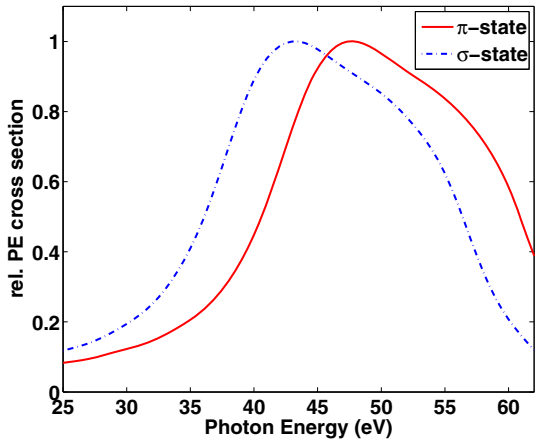

Fig. 5. Calculated relative cross section for photoemission from the σ and π bands of free standing graphene.

the ground state and the spectral bandwidth of the exciting photon source. The energy bandwidth of the occupied electronic states of graphene has been measured to be approximately 2 eV both for the π and the σ state [22] and it is assumed to be a Lorentzian function again. The spectral bandwidth of the high harmonic source is relatively broad due to the ultrashort pulse duration. A Gaussian spectral distribution with a FWHM of $\Delta E = 0.3$ eV has been measured. To calculate the relative PE cross sections for various photon energies under realistic experimental conditions, the density of states distribution in Figure 4 was convoluted with the energy distribution of the ground state and the spectral distribution of the photon source. Additionally, the ground state binding energy was taken into account. The resulting relative PE cross sections for the graphene σ and π states are plotted in Figure 5.

The calculated relative PE cross sections were normalized as in Figure 2 for a better comparison. The cross section dependence on photon energy is the same for emission from the σ and the π bands, because the same approximations were made for both states. The rising slope is slightly steeper than the falling slope when increasing the photon energy across the resonance. The overall shape of the calculated cross section resonances and their width in photon energies correspond well to the experimental data. The cross section for emission from the σ state reaches a maximum at a photon energy of $h\nu = 41$ eV, for emission from the π state a maximum at $h\nu = 46$ eV. The energetic shift between the maxima can simply be explained by the difference in binding energy of the two electronic states extracted from the tight-binding band structure calculations. However, the maxima of these resonances are shifted by about 5−7 eV to higher photon energies as compared to the experimental findings.

The tight-binding calculations have been performed for free standing graphene instead of graphene on a Ni(111) substrate. The energetic shift of the PE cross sections therefore reflects the signature of the interaction of the graphene with the nickel substrate which, as already stated in the results section, shifts the position of the σ and π bands by about 2 eV towards higher binding energies [16,17,23].

5 Conclusion

In this work we have experimentally and numerically investigated the PE cross section for graphene on Ni(111) up to photon energies of 54.6 eV. Resonances in the PE cross section were found for the graphene σ as well as the π state.

The measured PE cross sections were compared to a standard tight binding calculation for free standing graphene. A comparison between the calculated and the experimentally determined cross sections show a good qualitative agreement. The cross section resonances can therefore be explained by a high density of unoccupied electronic states in a small energy interval in $\Gamma \rightarrow L$ direction. The energetic shift between the calculated and measured maxima of the resonances is attributed to the effect of the interaction between the substrate and the graphene on the electronic structure.

This work was supported by the German Research Foundation (DFG) in the framework of the Priority Program 1459 (Graphene) and by the ‘Stichting voor Fundamenteel Onderzoek der Materie (FOM)’, which is financially supported by the Nederlandse Organisatie voor Wetenschappelijk Onderzoek (NWO).

References

1. K.S. Novoselov, A.K. Geim, S.V. Morozov, D. Jiang, Y. Zhang, S.V. Dubonos, I.V. Grigorieva, A.A. Firsov, Science **306**, 666 (2004)
2. A.K. Geim, Science **324**, 1530 (2009)
3. D.R. Cooper et al., ISRN Condensed Matter Physics **2012**, 56 (2012)
4. A.H. Castro Neto, F. Guinea, N.M.R. Peres, K.S. Novoselov, A.K. Geim, Rev. Mod. Phys. **81**, 109 (2009)

5. J. Wintterlin, M.L. Bocquet, Surf. Sci. **603**, 1841 (2009)
6. M. Batzill, Surf. Sci. Rep. **67**, 83 (2012)
7. A. Bostwick, T. Ohta, T. Seyller, K. Horn, E. Rotenberg, Nat. Phys. **3**, 36 (2007)
8. T. Pfeifer, C. Spielmann, G. Gerber, Rep. Prog. Phys. **69**, 443 (2006)
9. J. Hüve, T. Haarlammert, T. Steinbrück, J. Kutzner, G. Tsilimis, H. Zacharias, Opt. Commun. **266**, 261 (2006)
10. C. Spielmann, N.H. Burnett, S. Sartania, R. Koppitsch, M. Schnürer, C. Kan, M. Lenzner, P. Wobrauschek, F. Krausz, Science **278**, 661 (1997)
11. T. Haarlammert, H. Zacharias, Curr. Opin. Solid State Mater. Sci. **13**, 13 (2009)
12. C. Oshima, A. Nagashima, J. Phys.: Condens. Matter **9**, 1 (1997)
13. P. Jacobson, B. Stöger, A. Garhofer, G.S. Parkinson, M. Schmid, R. Caudillo, F. Mittendorfer, J. Redinger, U. Diebold, ACS Nano **6**, 3564 (2012)
14. A. Grüneis, K. Kummer, D.V. Vyalikh, New J. Phys. **11**, 073050 (2009)
15. S. Evans, J. Pielasze, J.M. Thomas, Surf. Sci. **55**, 644 (1976)
16. A. Grüneis, D.V. Vyalikh, Phys. Rev. B **77**, 193401 (2008)
17. Y.S. Dedkov, M. Fonin, New J. Phys. **12**, 125004 (2010)
18. J. Hermanson, Solid State Commun. **22**, 9 (1977)
19. A.R. Law, M.T. Johnson, H.P. Hughes, Phys. Rev. B **34**, 4289 (1986)
20. T. Haarlammert, A.V. Golovin, H. Zacharias, Phys. Rev. B **83**, 125435 (2011)
21. S. Reich, J. Maultzsch, C. Thomsen, P. Ordejón, Phys. Rev. B **66**, 035412 (2002)
22. T. Ohta, A. Bostwick, J.L. McChesney, T. Seyller, K. Horn, E. Rotenberg, Phys. Rev. Lett. **98**, 206802 (2007)
23. P.A. Khomyakov, G. Giovannetti, P.C. Rusu, G. Brocks, J. van den Brink, P.J. Kelly, Phys. Rev. B **79**, 195425 (2009)